

Title: Data-driven model of glycolysis identifies the role of allostery in maintaining ATP homeostasis

Authors: Mangyu Choe^{1,2}, Tal Einav^{4,6}, Rob Phillips^{4,5}, Denis V. Titov^{1,2,3*}.

Affiliations:

¹Department of Nutritional Sciences and Toxicology, University of California; Berkeley, CA 94720, USA.

²Department of Molecular and Cell Biology, University of California; Berkeley, CA 94720, USA.

³Center for Computational Biology, University of California; Berkeley, CA 94720, USA.

⁴Division of Biology and Biological Engineering, California Institute of Technology; Pasadena, CA 91125, USA.

⁵Department of Physics, California Institute of Technology; Pasadena, CA 91125, USA.

⁶Basic Sciences Division and Computational Biology Program, Fred Hutchinson Cancer Research Center, Seattle, WA 98109, USA.

*Corresponding author. Email: titov@berkeley.edu

Abstract: The specific roles of allostery in regulating metabolism are not well understood. Here, we develop a data-driven mathematical model of mammalian glycolysis that uses enzyme rate equations and coupled ordinary differential equations. The key components of our model are the rate equations for allosterically regulated enzymes based on the Monod-Wyman-Changeux model that we derive using a rigorous analysis of thousands of *in vitro* kinetic measurements. The resulting model recapitulates the properties of glycolysis observed in live cells and shows that the specific function of allosteric regulation is to maintain high and stable concentrations of ATP, while glycolysis without allosteric regulation is fully capable of producing ATP and ensuring that ATP hydrolysis generates energy. Our data-based modeling approach provides a roadmap for a better understanding of the role of allostery in metabolism regulation.

One-Sentence Summary: The glycolysis model based on allosteric enzyme rate equations recapitulates properties of glycolysis observed in live cells.

Main Text:

Glycolysis is conserved across all domains of life. This key pathway harnesses the breakdown of glucose to produce energy in the form of ATP and precursors for the biosynthesis of amino acids, nucleotides, carbohydrates, and lipids. Glycolysis contributes to ATP homeostasis by both directly producing ATP by a process referred to as fermentation or aerobic glycolysis (Fig. 1A) and by producing pyruvate that can be used as a substrate for additional ATP generation by mitochondrial respiration. Aerobic glycolysis is the most active metabolic pathway in proliferating mammalian cells (1) (an observation known as the Warburg Effect (2)), where it can satisfy all the ATP demand in the absence of respiration (3, 4). The net reaction of aerobic glycolysis converts extracellular glucose to two molecules of extracellular lactic acid, while the only net intracellular reaction is the production of ATP from ADP and inorganic phosphate (Fig. 1A). The reliance of proliferating cells on aerobic glycolysis for ATP production and the lack of intracellular products except for ATP makes glycolysis a convenient self-contained system for studying ATP homeostasis.

Glycolytic ATP production is regulated by mass action and a constellation of allosteric effectors that tune enzyme activity. Most of our knowledge about the allosteric regulation of glycolysis, and metabolism more broadly, is based on careful characterization of purified enzymes. However, the properties of metabolic pathways are the result of non-linear interactions between dozens of enzymes and metabolites, making it difficult to fully understand the global effects of regulation by studying enzymes in isolation. The production of glycolytic ATP provides a clear example of where our understanding falls short. While many allosteric regulators of glycolytic enzymes have been identified, we do not know what specific properties of glycolytic ATP production these molecules regulate. Properties of glycolytic ATP production include matching ATP supply and demand, maintaining ATP, ADP and phosphate concentrations such that ATP hydrolysis generates energy, maintaining a high concentration of ATP relative to ADP and AMP (5, 6), and enabling rapid adjustment of ATP production in response to changes in demand given the half-life of intracellular ATP as low as ~1-10 seconds (7). In addition, glycolytic ATP production has to coordinate with respiratory ATP production and with biosynthetic pathways. Currently, we do not know which of the latter properties of glycolysis require which allosteric regulators, and, in fact, we do not know which of these properties require allosteric regulation at all.

Due to the complexity of glycolytic ATP production, a better understanding of its regulation requires the use of mathematical modeling. This has been an active area of research for several decades, with many groups developing mathematical models of glycolysis (8–21). These efforts range from simple idealized models involving a subset of enzymes (8–10, 12, 16) to full-scale models containing all the enzymes (11, 13–15, 17–21). Previous studies had two key limitations that we wanted to address in this report. First, a systematic analysis of the requirement of allosteric regulators for various properties of glycolysis has not been performed. Second, enzyme rate equations used in the published models, especially for the allosterically regulated enzymes, were not systematically derived using comprehensive data from multiple *in vitro* kinetic studies.

Here we describe the development, analysis, and testing of a comprehensive model for the mammalian glycolytic pathway. Our model uses enzyme rate equations to describe glycolysis activity using a system of ordinary differential equations (ODEs). The key components of our model are the newly derived rate equations for allosterically regulated enzymes hexokinase (HK), phosphofructokinase (PFK), glyceraldehyde-3-phosphate dehydrogenase (GAPDH), and pyruvate kinase (PK). We use the Monod-Wyman-Changeux model (22–26) in combination with

rigorous statistical approaches to identify the relevant rate equations and to estimate the kinetic constants using a manually curated dataset of thousands of data points from dozens of publications. Our model recapitulates all the properties of glycolytic ATP homeostasis described above and accurately predicts absolute concentrations of glycolytic intermediates and isotope tracing patterns in live cells. We used the model to investigate the role of allosteric regulation in maintaining ATP homeostasis. Our analysis suggests that allosteric regulation is only required for the maintenance of high ATP levels in relation to ADP and AMP, while it is dispensable for other properties such as matching ATP supply and demand, ensuring that ATP hydrolysis generates energy, and enabling rapid adjustment of ATP production in response to changes in demand. Our analysis identifies the specific mechanism that allows allosteric regulation to maintain high ATP levels by controlling the rate of HK and PFK and shows that allosteric regulation is absolutely required for this property of glycolysis.

Results

Model development overview

We have developed a comprehensive mathematical model of aerobic glycolysis to understand the role of allostery in regulating ATP homeostasis. In this section, we provide an overview of the model development while most of the technical details are described in a comprehensive Supplementary Text, and Materials and Methods. Our model includes key allosteric regulators based on a thorough literature search. Most glycolytic enzymes are encoded by several homologous genes that produce enzyme isoforms with tissue-specific expression and distinct kinetic and allosteric properties. We chose to focus on glycolytic enzyme isoforms that are most abundant in proliferating cell lines to facilitate experimental testing (i.e., HK1, PFKP, and PKM2 isoforms of HK, PFK, and PK). We sought to develop a core model of glycolysis that supports ATP homeostasis in the absence of input from other pathways, and hence we only included allosteric regulators that are products or substrates of glycolytic enzymes. Our model converts a qualitative schematic of allosteric regulation (Fig. 1B) into a precise mathematical language. As input, the model uses *i*) the extracellular concentrations of glucose and lactate, *ii*) cellular concentrations of cofactor pools and glycolytic enzymes, and *iii*) the rate of cellular ATP consumption (Fig. 1C). We highlight these inputs separately from the model as these inputs are not controlled by glycolysis but depend on the cell type or experimental conditions and thus cannot be predicted by a glycolysis model. The model takes these inputs and uses enzyme rate equations assembled into a system of coupled ordinary differential equations (ODEs) to calculate the concentration of every glycolytic intermediate and the rate of every reaction. Our model can calculate both steady-state behavior and dynamical responses to perturbations. In effect, our model uses *in vitro* enzyme kinetics to predict any measurable property of glycolysis and many properties that cannot currently be measured.

In total, our model contains >150 parameters, including kinetic and thermodynamic constants, and estimates of enzyme and cofactor pool concentrations, yet all of these parameters are tightly constrained by experimental data. Kinetic constants were estimated from *in vitro* enzyme kinetics data as described briefly below and in full detail in the Supplementary Text. Thermodynamic constants are taken from the eQuilibrator database (27). Enzyme and cofactor pool concentrations are estimated from proteomics and metabolomics data, respectively, as described in Materials and Methods. We numerically simulate the model using DifferentialEquations.jl library (28) written in the Julia Programming Language (29). Our code is heavily optimized so that it takes ~1-10 milliseconds to calculate the results of the model under given conditions using a single core of a modern computer processor. Optimized code allows us

to run the model under millions of different conditions to systematically explore the regulation of glycolytic ATP homeostasis.

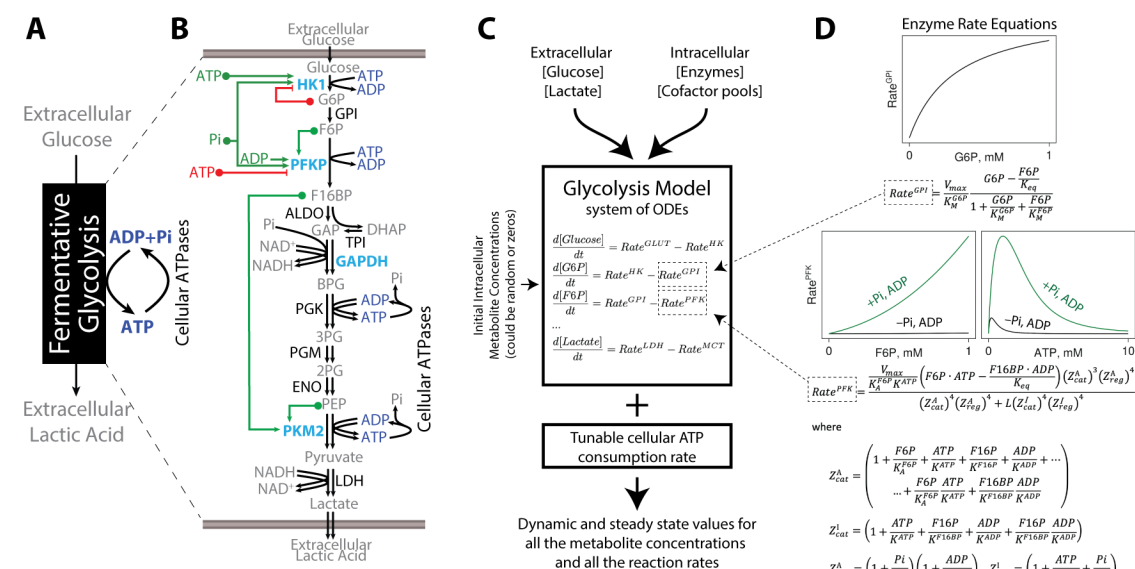


Fig. 1. Overview of the mammalian glycolysis model. (A) Coarse-grained description of aerobic glycolysis highlighting its main function to transform glucose into ATP. (B) Qualitative schematic of glycolysis showing the chain of enzymes (allosterically regulated enzymes in teal and the other enzymes in black) that convert substrates into products (gray). Allosteric activators (green) and inhibitors (red) that are included in the model are highlighted. (C) Schematic of the glycolysis model including inputs and outputs. (D) Kinetic rate equations are shown for GPI and PFK and plots are actual GPI and PFK rates calculated by the respective equations. Note the dramatic activation of the PFK rate in the presence of inorganic phosphate (Pi) and ADP.

The defining feature of our model is the use of newly derived kinetic rate equations to describe the activity of four allosterically regulated enzymes (i.e., HK1, PFKP, GAPDH, PKM2) using the Monod-Wyman-Changeux (MWC) model. MWC is a powerful model for describing the activity of allosterically regulated enzymes (22–26), which assumes that allosteric enzymes exist in two or more conformations with different kinetic properties. Both the binding of substrates and allosteric regulators can modify the kinetic properties of an MWC enzyme by stabilizing one conformation over another. We use statistical approaches (i.e., regularization and cross-validation) to identify the simplest MWC kinetic rate equation that can adequately describe the available data, allowing us to avoid overfitting and parameter identifiability issues common for fitting complex equations to finite data (30). MWC equation describing the rate of PFKP in the presence of substrates and regulators is shown in Fig. 1D. We described the rest of the glycolytic enzymes that are not believed to be allosterically regulated using standard kinetic rate equations derived from quasi-steady-state or rapid equilibrium approximations. For the eight enzymes and transporters with one substrate and one product, we used reversible Michaelis-Menten equations (see equation describing the rate of glucose-6-phosphate isomerase (GPI) in Fig. 1D) and estimated their kinetic constants by averaging values from at least three publications per constant to verify their consistency and accuracy. For the three remaining enzymes with more than one substrate or product (i.e., aldolase (ALDO), phosphoglycerate kinase (PGK), and lactate dehydrogenase (LDH)), we fitted their more complex rate equations to manually curated *in vitro* kinetics datasets containing 350-700 data points per enzyme. We chose to fit data from ALDO, PGK, and LDH instead of averaging over published kinetic constants because many publications

describing ALDO, PGK, and LDH activity used different rate equations, and hence the published kinetic constants are not directly comparable. A comprehensive description of the derivations and fitting of all enzyme rate equations is reported in the Supplementary Text, and we hope this compendium of information will serve as a great resource for future investigations of these enzymes.

Finally, we want to highlight that our model uses several assumptions that have to be considered when interpreting its predictions. First, the model assumes that the activity of enzymes in living cells is accurately described using *in vitro* activity of purified enzymes. Second, the model assumes that enzymes and metabolites are well-mixed in the cytosol of the cell. Third, the model only describes the effect of regulators that are included in the model. Fourth, the model assumes that other pathways (e.g., pentose phosphate pathway, mitochondrial pyruvate consumption) do not affect the concentration of glycolytic intermediates or glycolytic reaction rates. Deviations between the model and experimental observations could be due to any number of these assumptions not being valid under the conditions of a particular experiment. On the other hand, if the model accurately predicts experimental data, it suggests that these assumptions are valid under given experimental conditions.

Glycolysis model recapitulates key properties of ATP homeostasis

After constructing the model, we first investigated whether it can recapitulate the three key properties of ATP homeostasis observed in living cells. First, a minimal working model must match ATP supply and demand. Second, it should maintain a high ATP concentration such that most of the adenine nucleotide pool is in the form of ATP at a wide range of ATP turnovers as observed *in vivo* (5, 6). Third, the model should maintain the mass-action ratio of ATP hydrolysis reaction (i.e., the ratio of product concentrations [ADP]•[Phosphate] to substrate concentrations [ATP]) far from equilibrium, which is what allows ATP to drive energy-demanding processes in the cell.

We performed simulations to determine whether the glycolysis model can recapitulate the key properties of ATP homeostasis. We report all ATPase rates in terms of percent of HK1 activity, which is the slowest enzyme and glycolysis cannot proceed faster than the maximal rate of its slowest enzyme (maximal rates are determined by the product of intracellular enzyme concentration and V_{max}). First, we found that the glycolysis model produces as much ATP as is consumed and rapidly adjusts to stepwise increase or decrease of ATP consumption, as is necessary under physiological conditions (Fig. 2A). Second, we showed that > 90% of adenine nucleotide pool was maintained as ATP and ATP concentrations varied by < 10% when we introduced physiologically relevant 2-fold stepwise changes in ATP consumption rate (Fig. 2B). Thus, as has been observed in muscle and heart *in vivo* (5, 6), our model maintains nearly constant ATP levels in response to large changes in ATP turnover. The latter is the key property of feedback regulation of glycolysis that is required to ensure that cellular ATP-consuming enzymes with $K_M \sim 1$ -100 μ M are not affected by changes in ATP turnover. Finally, we showed that the glycolysis model maintains ATP, ADP and inorganic phosphate concentrations such that the ATP hydrolysis reaction is 10^9 - 10^{11} -fold away from equilibrium, equivalent to 20-25 $k_B T$ (Fig. 2C), which is similar to what has been measured in cells (7) and what allows ATP hydrolysis to drive energy-demanding processes. We reran the model 10,000 times using randomly drawn model parameters and initial conditions to show that the ability of the model to maintain most of the adenine nucleotide pool in the form of ATP levels is largely insensitive to initial conditions and to changes in model parameters within the range of experimental errors for each parameter (Fig. S1). The coefficient of variation (CV) of the area under the curve of ATP

concentrations at a range of ATPase rates (15%) is lower than the average CV of a model parameter (24%), which suggests that maintenance of high ATP levels is the robust property of the model (Fig. S1B).

Several kinetics models of glycolysis have been reported over the past several decades, yet none of these reports investigated whether those models can recapitulate properties of ATP homeostasis except for matching ATP supply and demand. To perform a head-to-head comparison, we implemented a recent mechanistic model of yeast glycolysis that we will refer to as the van Heerden model (19). Upon repeating the simulations in Fig. 2A-C (Fig. S2), the van Heerden model produced ATP in response to ATP consumption and maintained the high energy of ATP hydrolysis (Fig. S2A, C). However, the van Heerden model could only support ATP levels that are orders of magnitude lower than our model and exhibited volatility in ATP concentration spanning almost two orders of magnitude in response to 2-fold stepwise changes in ATP demand compared to the <10% change exhibited by our model under the same conditions (Fig. S2B). Thus, the van Heerden model does not capture the feedback regulation that is needed to maintain most of the adenine nucleotide pool in the form of ATP and ensure stable ATP levels in response to changes in ATPase rate as observed *in vivo* (5, 6).

In summary, our glycolysis model is the first reported model that recapitulates all the key properties of ATP homeostasis such as matching ATP supply and demand, maintaining stable ATP levels such that most of the adenine nucleotide pool is in the form of ATP, and maintaining high energy of ATP hydrolysis over a large range of ATP consumption rates.

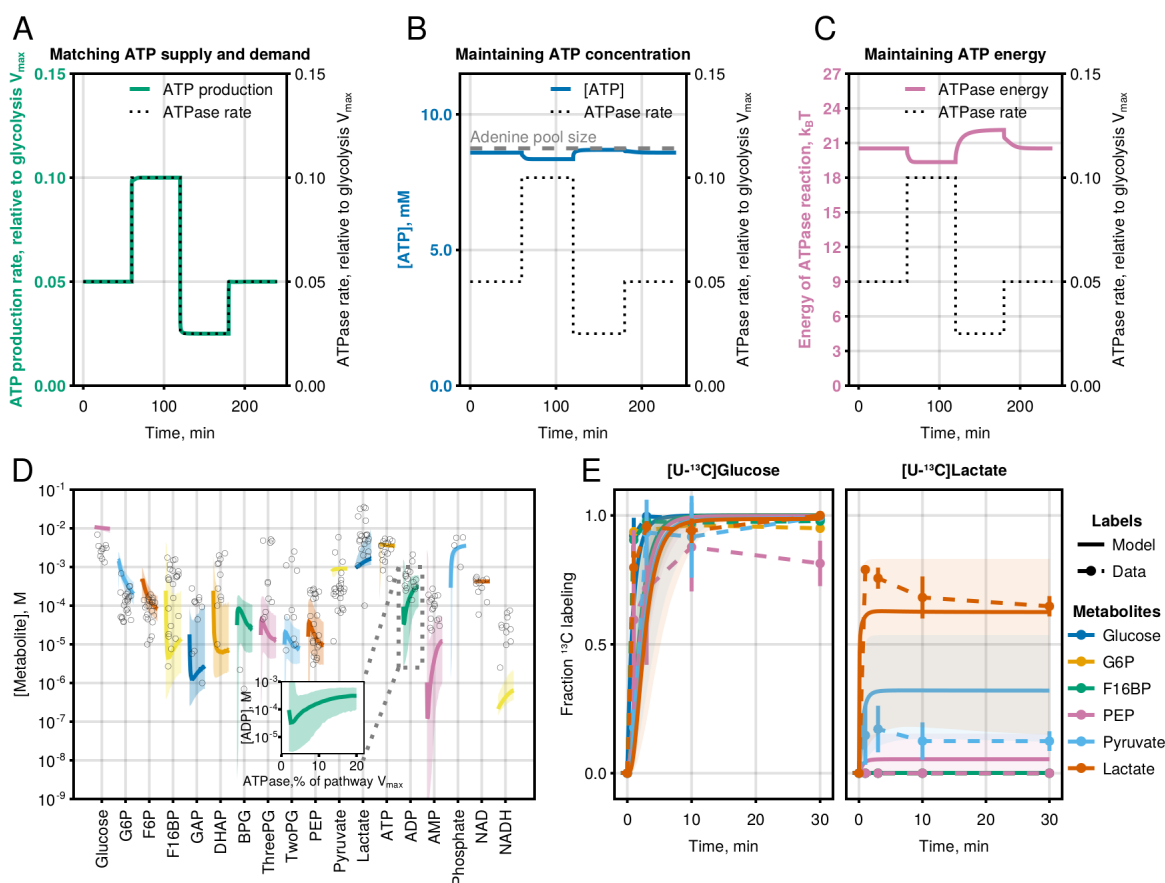


Fig. 2. Glycolysis model recapitulates qualitative and quantitative properties of glycolysis observed in live cells.

(A-C) Model simulations showing changes in (A) ATP production rate, (B) ATP concentration (total adenine pool size is labeled with dashed grey line), and (C) energy released during ATP hydrolysis in response to a 2-fold stepwise increase or decrease of ATPase rate. ATPase energy is calculated as a natural logarithm of the disequilibrium ratio (i.e., mass-action ratio divided by the equilibrium constant) for the ATPase reaction. (D) Comparison of measured glycolytic intermediate concentrations and model predictions. Black empty circles indicate the experimentally determined metabolite concentrations. Colored lines with ribbon indicate the median and 95% CI of model predictions. The shift from left to right for each metabolite level prediction corresponds to increasing rates of ATP consumption from 2% to 20% of glycolysis V_{max} (see inset for ADP) to highlight the effect of ATP consumption on metabolite concentrations. (E) Comparison of $[U-^{13}C]$ Glucose and $[U-^{13}C]$ Lactate tracing data with model prediction. Circles connected with dotted lines are data and lines with ribbons are model predictions. ATPase rate = 15% of glycolysis V_{max} was chosen for model predictions. Model predictions in (D) and (E) are from simulations where bootstrapped model parameter combinations could match ATP supply and demand, which were > 79% and >93% of simulations for (D) and (E), respectively. Julia code to reproduce this figure is available at <https://github.com/DenisTitovLab/Glycolysis.jl>.

Glycolysis model recapitulates live cell data

Given that our model could reproduce the wealth of measurements of each glycolytic enzyme *in vitro* and recapitulate the key properties of ATP homeostasis, we set out to determine whether the model could predict the results of experiments in live cells.

To directly compare model predictions to data from bulk cell measurements, we had to adjust the model output in two ways. First, we corrected for the fact that metabolites inside the cell can either be bound to proteins or exist in free form in solution. Concentration terms in enzyme rate equations refer specifically to free metabolite concentrations, so we converted free metabolite concentrations to free + bound concentrations (using the known concentrations and binding constants of all enzymes) before comparing prediction to bulk cell lysis measurements. An important caveat of this calculation is that we only consider glycolytic enzymes, which neglects the binding of glycolytic intermediates to other enzymes. Second, we corrected for the fact that glycolytic enzymes are localized to the cytosol (i.e., the part of the cytoplasm that is devoid of organelles) and that a significant fraction of cytosol is occupied by macromolecules and not water. The latter effectively means that all the enzymes and metabolites of glycolysis are concentrated in a volume that is ~50% of cellular volume assuming 70% of the cell is cytosol and 70% of the cytosol is water.

We first compared the model predictions of bound and free metabolites with absolute intracellular metabolite concentrations determined by liquid chromatography-mass spectrometry (LC-MS). Mammalian cells can synthesize ATP using the mitochondrial electron transport chain (ETC) or aerobic glycolysis. Since our current model only describes ATP homeostasis by aerobic glycolysis, the most appropriate comparison would be with cells that don't have a functional ETC like red blood cells (which do not have mitochondria and get their ATP exclusively from aerobic glycolysis) or cells treated with ETC inhibitors. In our experiments, we opted for the latter, performing our experiments in the presence of ETC inhibitors. Yet, in addition, we also used published data from red blood cells as well as cancer cell lines because the model predictions suggested that the effect of glycolysis rate on the concentrations of most

intermediates is smaller than the confidence intervals of model predictions. Indeed, we found that 95% confidence intervals of model predictions of most of the 18 glycolytic intermediate concentrations at a range of ATP consumption rates overlapped within experimental values (Fig. 2D). The latter result is notable given that our model contains no direct information about intracellular metabolite levels and is free to predict concentrations from 0 to $+\infty$ and even below zero if the model is implemented incorrectly.

Next, we compared [U- ^{13}C]Glucose and [U- ^{13}C]Lactate labeling kinetics predicted by the model and measured in experiments. For these measurements, we exchanged normal media for media containing [U- ^{13}C]Glucose (the input for the glycolysis pathway) or [U- ^{13}C]Lactate (the final product) and then lysed cells at different time intervals to estimate the rate and fraction at which ^{13}C from [U- ^{13}C]Glucose or [U- ^{13}C]Lactate is incorporated into glycolytic intermediates. We observed that the glycolysis model accurately recapitulated the kinetics of ^{13}C labeling fraction of intermediates after switching to [U- ^{13}C]Glucose or [U- ^{13}C]Lactate-containing media (Fig. 2E). It is particularly noteworthy that the model can recapitulate labeling from [U- ^{13}C]Lactate where only intracellular lactate and pyruvate are labeled, as this indicates that our model can accurately capture the extent of *reversibility* of glycolysis reactions.

Allosteric regulation of HK1 and PFKP is required for the maintenance of ATP levels

Having established that the model recapitulates the key properties of ATP homeostasis and accurately predicts measurement in live cells, we next used the model to investigate the function of allosteric regulation in maintaining ATP homeostasis. We hypothesized that specific allosteric regulators could serve in a number of critical roles including matching ATP supply and demand, maintaining high and stable ATP levels such that the majority of the adenine nucleotide pool is in the form of ATP, rapidly responding to acute perturbations of the ATPase rate, or maintaining high energy of ATP hydrolysis.

We first removed all allosteric regulators to see if the resulting simple pathway remained functional. Specifically, we made the HK1, PFKP, GAPDH, and PKM2 enzymes behave as Michaelis-Menten-like enzymes with kinetic parameters corresponding to their faster (active) MWC conformation. We also removed competitive inhibition of the HK catalytic site by G6P, which proceeds through standard non-allosteric competitive inhibition. Surprisingly, the model without any regulation was fully capable of matching ATP supply and demand and was further able to maintain the high energy of ATP hydrolysis (Fig. 3A, C). However, without allosteric regulation, we observed a complete breakdown of ATP concentration maintenance, where ATP levels were almost 1000-fold lower, and a small 2-fold increase and decrease of ATPase rate led to an almost 10-fold change in ATP concentration compared to <10% change in ATP concentration for the complete model (Fig. 3B). Allosteric regulation allowed glycolysis to maintain >90% of the adenine pool in the form of ATP while in the absence of allosteric regulation <1% of the adenine pool was in the form of ATP. Systematic investigation of model behavior at different ATPase rates showed that the model without regulation is not capable of maintaining most of the adenine nucleotide pool in the form of ATP levels at any ATPase value, which is contrary to the constant ATP concentrations observed both *in vivo* (5, 6) and in the complete model (Fig. 3D, vertical drop-off indicates where the ATP production by the model cannot match ATPase rate anymore). We also note that the unregulated model can support higher ATP production rates hinting at the potential tradeoffs of maintaining high ATP level using allosteric regulation (Fig. 3E, solid red line is shifted to the right of the solid blue line).

We next removed the regulation of specific enzymes one by one, computationally dissecting the pathway to better understand the role of each enzyme (Fig. 3D-F, Fig. S3). Specifically, we removed a particular allosteric regulator from the relevant kinetic rate equations by setting its binding constant for both active and inactive MWC conformation to ∞ . We found that the allosteric regulation of HK1 and PFKP is responsible for maintaining high and stable ATP levels, whereas removing the allosteric regulation of GAPDH and PKM2 had no discernable effect (Fig. 3D). Digging further, we removed each of the allosteric activators and inhibitors of HK1 and PFKP and found that these regulators work together to ensure the robust maintenance of ATP levels, so that removing any single regulator only led to a partial loss of ATP maintenance capacity (Fig. S3). In general, removing inhibitors (i.e., G6P for HK1 and ATP for PFKP) led to worse ATP maintenance at low ATPase rates (Fig. 3E, Fig. S3E-H), while removing activators (i.e., phosphate for both HK1 and PFKP and ADP for PFKP) led to poorer ATP maintenance at high ATPase rates (Fig. 3F, Fig. S3K-N).

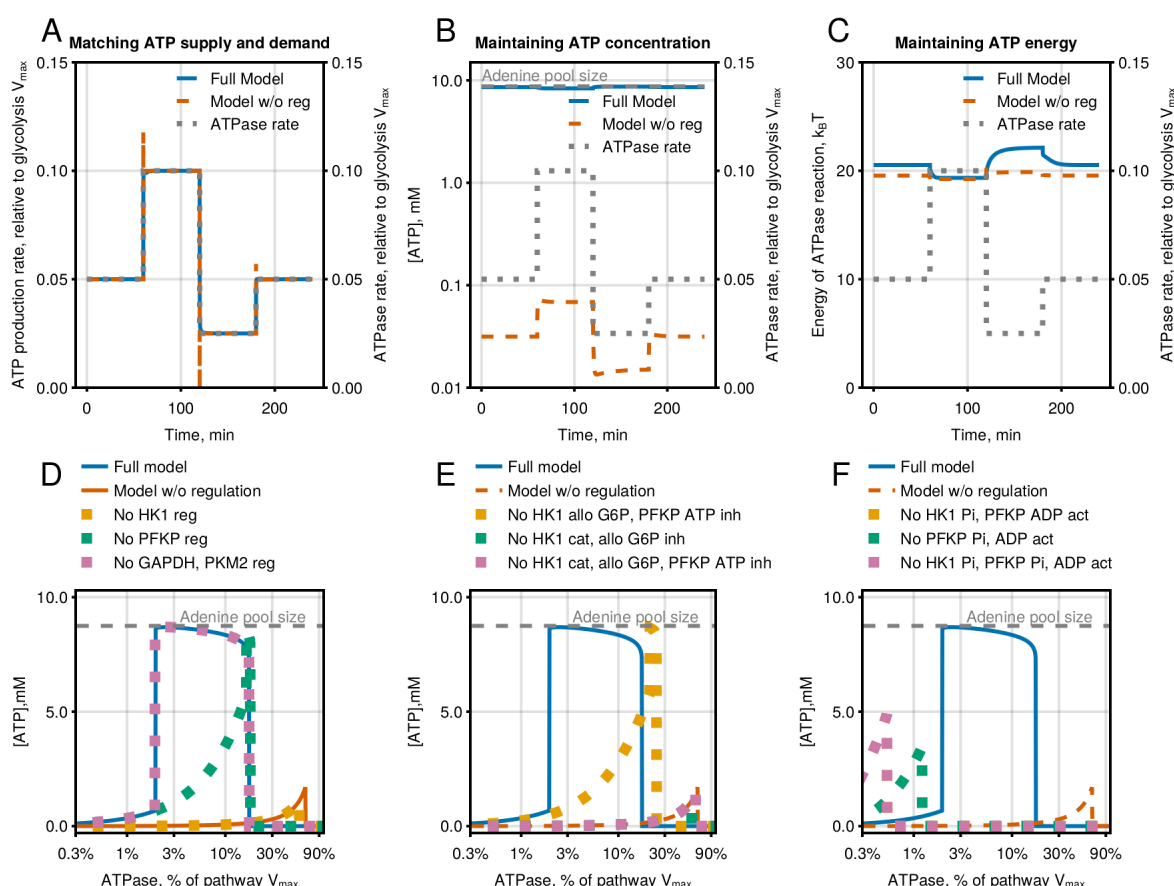


Fig. 3. Allosteric regulation is required for the maintenance of high and stable ATP levels. (A-C) Model simulations showing the effect of removal of allosteric regulation of HK1, PFKP, GAPDH, and PKM2 on (A) ATP production rate, (B) ATP concentration, and (C) energy released during ATP hydrolysis [Left axis] in response to a 2-fold stepwise increase or decrease of ATPase rate [Right axis]. Energy is calculated as a natural logarithm of the disequilibrium ratio (i.e., mass-action ratio divided by the equilibrium constant) for the ATPase reaction. (D-F) Steady-state ATP concentrations at a range of ATPase rate of the glycolysis model with and without (D) allosteric regulation of enzymes, (E) allosteric activators, and (F) allosteric

inhibitors. Dashed grey line indicates the total adenine pool size (i.e., ATP + ADP + AMP). Julia code to reproduce this figure is available at <https://github.com/DenisTitovLab/Glycolysis.jl>.

We performed a global sensitivity analysis of our model to systematically explore the role of all model parameters in matching ATP supply and demand, maintaining high ATP levels, and maintaining high energy of ATP hydrolysis. The goal of global sensitivity analysis is to calculate the contribution of each model parameter and parameter interactions to the variance of a specific model output (31). We used the area under the curve (AUC) for the ratio of ATP production to ATP consumption, the ratio of ATP concentration to adenine pool size, and the energy of ATP hydrolysis at a log range of ATPase values as proxies for the model's ability to match ATP supply and demand, maintain high ATP levels and maintain high energy of ATP hydrolysis, respectively (Fig. S4A, D, G). We first estimated the variance of the AUC proxies by randomly varying each parameter of the model independently from a uniform distribution spanning a 9-fold range from 3 times lower to 3 times higher than the default model parameter values. The coefficient of variation for all three AUC proxies was in the narrow range of 0.13-0.4 in response to random changes in parameter values spanning 9-fold, indicating that these are robust properties of the model (Fig. S4B, E, H). The coefficient of variation for maintaining high ATP levels was about 3-fold larger than for maintaining high energy of ATP hydrolysis or for matching ATP supply and demand, suggesting that the former is more sensitive to changes in specific model parameters. Two metrics for each model parameter are typically reported for variance-based global sensitivity analysis. The first-order effect sensitivity index S_I reports the fraction of variance of the model output that will be removed if the corresponding parameter is fixed. The total-order sensitivity index S_T reports the variance that will be left if values of all but the corresponding parameter are fixed. Larger values of S_I and S_T indicate that a given parameter is important. Global sensitivity analysis showed that the K_M and V_{max} for HK1 had the highest S_I and S_T for all three model outputs, as expected since HK1 is the rate-limiting enzyme in the pathway. The second largest S_I and S_T for maintaining high ATP levels were given by the kinetic parameters that control allosteric regulation of HK1 and PFKP while the second largest S_I and S_T for matching ATP supply and demand and for maintaining high energy of ATP hydrolysis were simply the K_M and V_{max} of PFKP or the second slowest enzyme in the model after HK1 based on the product of enzyme concentration and V_{max} (Fig. S4C, F, I).

In summary, analysis of our model proposes that the function of allosteric regulation of HK1 and PFKP is to maintain high and stable ATP levels, while a pathway composed of non-allosteric, unregulated enzymes is sufficient to rapidly produce ATP in response to ATP consumption and maintain high energy of ATP hydrolysis.

Mechanism of high and stable ATP level maintenance by HK1 and PFKP allosteric regulation.

We next wanted to gain insight into the mechanism by which allosteric regulation of HK1 and PFKP allows glycolysis to maintain high and stable ATP levels. Here, we first provide an intuitive explanation of the mechanism that we identified and then show simulations supporting this mechanism. The concentration of ATP inside the cell is limited by adenine nucleotide pool size. To maintain a high ATP level, glycolysis has to convert most of the ADP into ATP or, equivalently, maintain most of the adenine nucleotide pool in the form of ATP. The latter automatically leads to the ability of glycolysis to maintain near-constant ATP levels in a narrow range of <10% (or <1%) at a range of ATP turnover rates where glycolysis can maintain >90% (or >99%) of adenine nucleotide pool as ATP. The relative level of ATP and ADP concentrations depends on the kinetic properties of ATP-consuming enzymes HK1 and PFKP and ATP-

producing enzymes PGK and PKM2. ATP consumption rate by the cell is of course another key determinant of ATP and ADP levels but this reaction is not directly controlled by glycolysis. Reactions in a metabolic pathway can proceed at the same arbitrary rate of 1 while being far from equilibrium (i.e., forward reaction rate of 1 and reverse rate of 0) or close to equilibrium (i.e., forward rate of 101 and reverse rate of 100). Under the conditions when glycolysis proceeds in the net forward direction, the concentrations of products relative to substrates for each enzyme will be highest if the enzyme reaction is close to equilibrium and lowest if the enzyme reaction is far from equilibrium. Therefore, to maintain a high level of ATP in relation to ADP glycolysis has to maintain ATP-consuming enzymes (i.e., ATP is a substrate and ADP is the product) HK1 and PFKP as far from equilibrium as possible and ATP-producing enzymes (i.e., ADP is a substrate and ATP is the product) PGK and PKM2 as close to equilibrium as possible (Fig. 4A). The above is the general consequence of the structure of the glycolysis pathway that has both ATP-consuming and ATP-producing reaction and is independent on the specific kinetic properties of enzymes. Simulations show that the glycolysis model behaves according to the principle described above where HK1 and PFKP reaction are kept much further from equilibrium (forward to reverse rate ratio of 10^6 - 10^8) than all other glycolytic enzymes at a range of ATPase rates that support high levels of ATP (Fig. 4B).

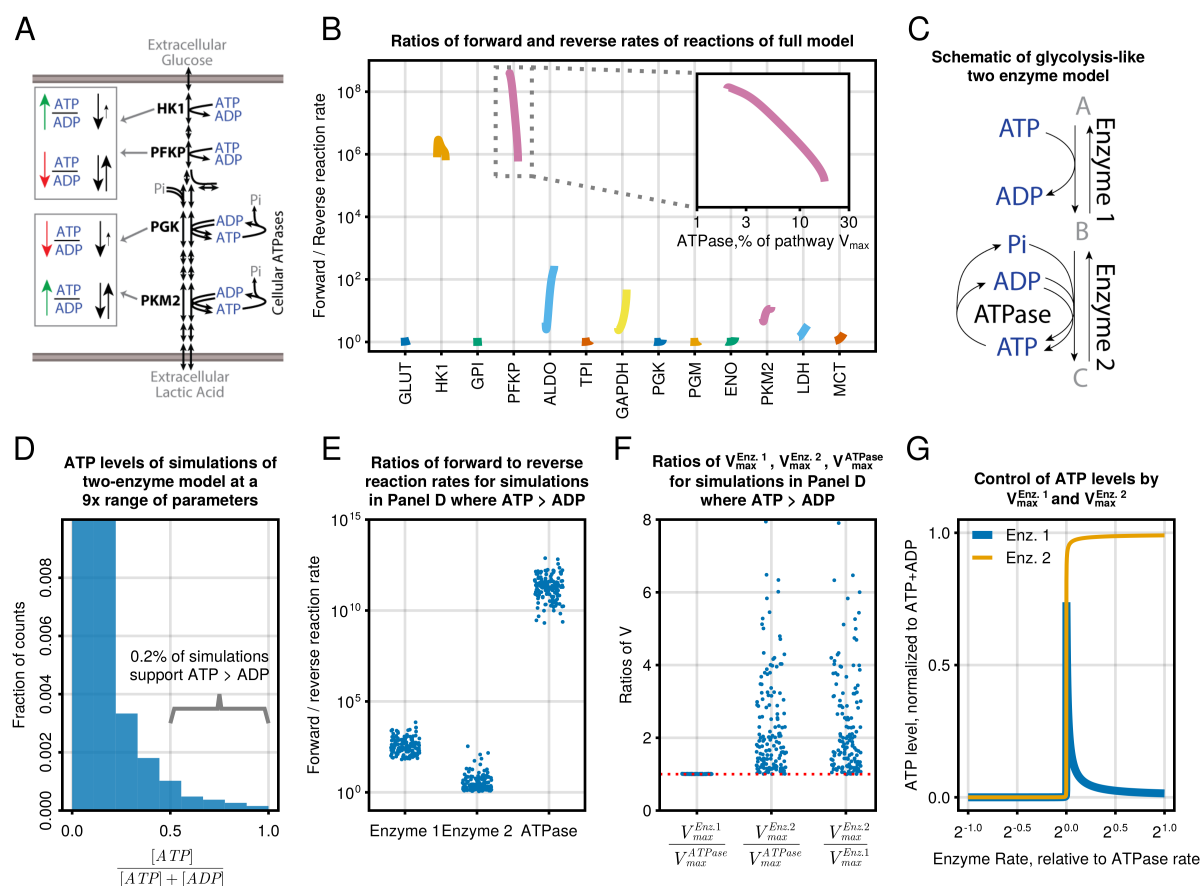
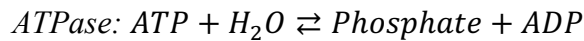
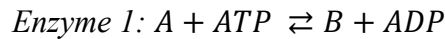


Fig. 4. Allosteric regulation maintains high ATP levels by keeping ATP-consuming HK and PFK reactions far from equilibrium at a range of ATP turnovers. (A) Schematic of the glycolysis pathway showing that in order to maintain high ATP level HK and PFK reactions should be far from equilibrium and PGK and PK close to equilibrium. **(B)** Ratio of forward to

reverse rate for all enzymes in the full model at a range of ATPase that support high ATP level showing that HK and PFK are maintained far from equilibrium. Data for each enzyme is displayed at a 2-20% range of increasing ATPase rates from left to right as shown in more detail in the inset. (C) Schematic of a simplified glycolysis-like pathway containing two enzymes. (D) Simulation of the two enzyme pathway at 9-fold range of the 6 parameter controlling this pathway showing that only ~0.1% of parameter combination support conditions when ATP > ADP. (E) Ratio of forward to reverse rates for Enzyme 1, Enzyme 2 and ATPase of two enzyme model for simulations in Panel D that support ATP > ADP. (F) Ratios of $V_{max}^{Enz\ 1}$, $V_{max}^{Enz\ 2}$ and V_{max}^{ATPase} of two enzyme model for simulations in Panel D that support ATP > ADP. (G) Simulation of two enzyme model ($K_{eq}^{Enz\ 1} = K_{eq}^{Enz\ 2} = 100$ and $K_{eq}^{ATPase} = 1000$) shows that maximal ATP level is achieved when rate of Enzyme 1 is exactly equal to rate of ATPase and rate of enzyme 2 is higher than ATPase rate. Julia code to reproduce this figure is available at <https://github.com/DenisTitovLab/Glycolysis.jl>.

To gain a better understanding of how glycolysis maintains high ATP levels, we used a simplified model of glycolysis, referred to as two-enzyme model, containing ATP-consuming Enzyme 1, ATP-producing Enzyme 2 and ATPase (Fig. 4C):



Note that metabolite B is phosphorylated, which conserves phosphate in each step. We describe the rates of Enzymes 1 and 2 and ATPase using a simple mass-action driven equation with two parameters being the maximal enzyme activity V_{max}^{Enz} (superscripts always denote the enzyme under consideration) and the equilibrium concentration of reaction K_{eq}^{Enz} :

$$Rate^{Enz} = V_{max}^{Enz} \left(1 - \frac{\Gamma^{Enz}}{K_{eq}^{Enz}} \right) \quad (1)$$

where Γ^{Enz} is the mass action ratio of corresponding reaction:

$$\begin{aligned} \Gamma^{Enz\ 1} &= \frac{[B][ADP]}{[A][ATP]} \\ \Gamma^{Enz\ 2} &= \frac{[C][ATP]^2}{[B][ADP]^2[Phosphate]} \\ \Gamma^{ATPase} &= \frac{[ADP][Phosphate]}{[ATP]} \end{aligned}$$

The two-enzyme model reduces the number of parameters from > 100 to 6. Only two of the parameters of the two-enzyme model can be controlled by allostery ($V_{max}^{Enz\ 1}$ and $V_{max}^{Enz\ 2}$), further simplifying the analysis of the role of allostery in regulating this model.

We first searched for values of the six parameters of the two-enzyme model that would support ATP > ADP. We performed 100,000 simulations using random values of all 6 parameters drawn from uniform distribution spanning a 9-fold range from 3 times lower to 3 times higher than then default model parameters $V_{max}^{Enz\ 1} = V_{max}^{Enz\ 2} = V_{max}^{ATPase} = 0.001$, $K_{eq}^{Enz\ 1} = K_{eq}^{Enz\ 2} = 100$, and $K_{eq}^{ATPase} = 1000$ (Fig. 4D). Only ~ 0.1% of parameter combinations could maintain ATP >

ADP. By contrast, ~25% of simulations could match ATP supply and demand or maintained energy of ATP hydrolysis above 10 k_BT, suggesting that maintenance of ATP > ADP is a non-trivial task that requires specific combinations of the 6 parameters (Fig. S5A, D).

We investigated the parameter combinations that allowed the two-enzyme model to maintain ATP > ADP. The simulations that supported ATP > ADP also maintained Enzyme 1 and ATPase reaction far from equilibrium and Enzyme 2 reaction close to equilibrium (Fig. 4E) as is described for the full glycolysis model above. We next investigated the ratios of parameters that allowed the two-enzyme model to maintain ATP > ADP, and we found a simple relationship $V_{max}^{Enz\ 2} > V_{max}^{Enz\ 1} = V_{max}^{ATPase}$ (Fig. 4F). We confirmed this relationship in simulations where we fixed $V_{max}^{Enz\ 1} = V_{max}^{ATPase}$ or $V_{max}^{Enz\ 2} = V_{max}^{ATPase}$ and varied the rate of the other enzyme (Fig. 4G). On the other hand, any condition where $V_{max}^{Enz\ 1} > V_{max}^{ATPase}$ and $V_{max}^{Enz\ 2} > V_{max}^{ATPase}$ was sufficient to match ATP supply and demand or to maintain high energy of ATP hydrolysis (Fig. S5B, C, E, F). Overall, our analysis suggests that to maintain high and stable ATP levels, allosteric regulation has to keep HK1 and PFKP reactions far from equilibrium by controlling the apparent V_{max} rates of these enzymes such that they are exactly equal to each other and to the apparent V_{max} of ATPase rate while being lower than the rates of all other glycolytic enzymes at a range of ATPase rates.

Excess activity of enzymes relative to HK and PFK is required for the maintenance of ATP levels

We next explored what attributes of the glycolysis pathway other than allosteric regulation of HK1 and PFKP might be required for maintaining most of the adenine pool in the form of ATP. Analysis of the two-enzyme model showed that the activity of ATP-producing Enzyme 2 should be as high as possible compared to the activity of ATP-consuming Enzyme 1 and ATPase (Fig. 4G). We investigated whether a similar mechanism works in the full glycolysis model. First, we looked at the maximal activity of glycolytic enzymes. In agreement with the two-enzyme model, most glycolytic enzymes have a large excess of activity compared to HK1 and PFKP (Fig. 5A). In fact, most enzymes are present at 10-fold higher concentrations than is required for the maximal activity of the glycolysis pathway limited by HK1. Such high levels of expression represent a significant investment of resources by the cell, given that expression of enzymes like GAPDH and PKM2 can approach 1% of the proteome.

Using our model, we tested whether this high level of enzyme expression is required to maintain high ATP levels. Increasing or decreasing the concentrations of all enzymes from TPI to LDH by 20-fold more than default model values led to no changes in ATP maintenance (Fig. 5B). However, upon decreasing the expression of these enzymes more than 20-fold, the ability of the model to maintain more than 50% of the adenine pool in the form of ATP levels eventually collapsed (Fig. 5B) without significantly affecting the ability of the model to match ATP supply and demand (Fig. 5C). In this way, our results suggest a mechanistic explanation for the seemingly wasteful large excess expression of enzyme of glycolysis relative to HK and PFK.

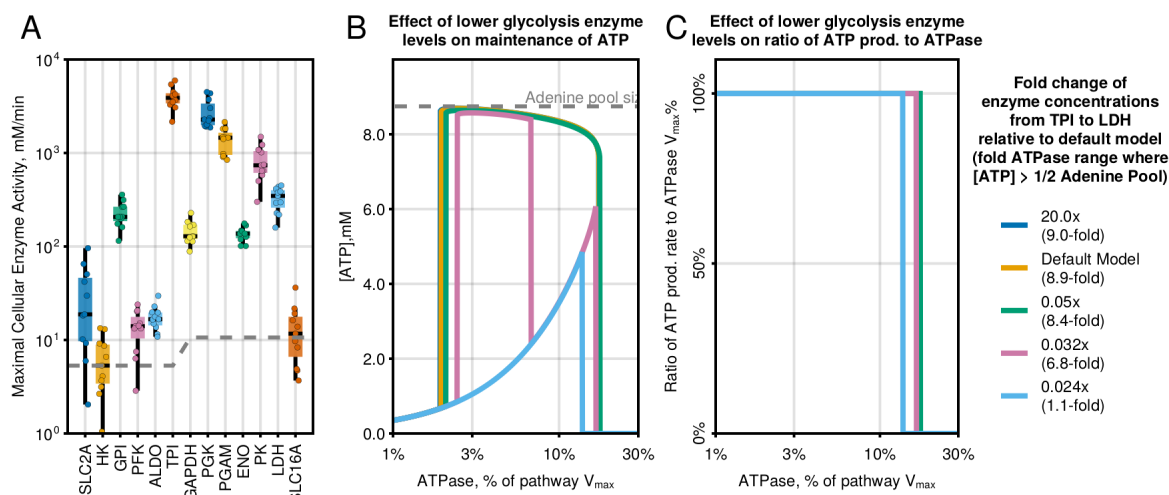


Fig. 5. Excess activity of glycolytic enzymes relative to HK and PFK is required for ATP maintenance. (A) Maximal enzyme activity in the model. Activities of all isoforms for each enzyme were summed together. The dashed line indicates the activity for each enzyme that matches the maximal activity of the slowest enzyme HK1 corrected for the stoichiometry of reactions. (B) Steady-state ATP concentrations at a range of ATPase rates of the glycolysis model with scaled concentrations of lower glycolysis enzymes TPI, GAPDH, PGK, PGAM, ENO, PK, and LDH. The dashed grey line indicates the total adenine pool size (i.e., ATP + ADP + AMP). The fold range of ATPase rates where the model can maintain >50% of the adenine nucleotide pool as ATP is highlighted in legend. (C) Ratios of ATP production rate to ATPase V_{max} at a range of ATPase rates of the glycolysis model with scaled concentrations of lower glycolysis enzymes TPI, GAPDH, PGK, PGAM, ENO, PK, and LDH. Julia code to reproduce this figure is available at <https://github.com/DenisTitovLab/Glycolysis.jl>.

Inorganic phosphate pool improves the maintenance of high ATP levels

We next investigated the role of cofactor pool sizes in maintaining ATP levels. The three cofactor pools that are included in our model are the adenine nucleotide pool (i.e., ATP+ADP+AMP), NAD(H) pool (i.e., $\text{NAD}^+ + \text{NADH}$), and the inorganic phosphate pool (i.e., the sum of all phosphate atoms except for ATP, ADP, and AMP). For the inorganic phosphate pool, we chose not to consider phosphate which is part of the adenine nucleotide pool to be able to separate the effect of inorganic phosphate and the effect of adenine nucleotides. We performed a global sensitivity analysis by varying cofactor pool sizes over a 9-fold range centered around the default values of each pool size. Based on S_I and S_T sensitivity indexes, phosphate pool size had the largest effect on the model's ability to maintain high ATP levels while adenine pool size had a smaller effect and NAD(H) pool size had little to no effect (Fig. S6A-B).

To confirm the effect of the phosphate pool on maintaining ATP levels, we simulated an increase or decrease of the level of all phosphorylated metabolites except ATP, ADP, and AMP (Fig. 6A). The simulations showed that doubling the phosphate pool led to an increase in the range of ATPase rates where the model can maintain more than 50% of the adenine pools in the form of ATP (i.e., faster divided by slowest supported ATPase rate) from 9-fold to 19-fold. While removal of the phosphate pool led to the shrinking of the supported ATPase range from 9-fold to 1.3-fold. This effect is ultimately driven by the concentration of inorganic phosphate, which if

kept constant abrogates the effect of a changing phosphate pool (Fig. S6C) and largely rescues high ATP level maintenance at low ATPase rates. This suggests that at low ATPase rates, our model is not capable of keeping phosphate concentration high enough to allow sufficient GAPDH activity as a large fraction of phosphate is incorporated into glycolytic intermediates. The phosphate pool of the default model is ~20mM, which, based on our simulations, is large enough to achieve close to optimal ATP level maintenance for our model (Fig. 6A). Cells have several reserves for phosphate in addition to glycolytic intermediates such as creatine phosphate and phosphorylated nucleotides other than adenines, which together contribute to at least 10 mM additional phosphate pool. In addition, cells have complex regulatory machinery to regulate intracellular phosphate levels, and it is likely that this machinery will prevent phosphate concentration from dropping below the minimal level sufficient for GAPDH activity. The inclusion of these additional phosphate reserves and phosphate regulatory systems should further improve the ATP level maintenance of our model and might fully eliminate the defect observed at low ATPase rates.

Finally, we confirmed the effect of adenine pool size on ATP level maintenance using simulations where we increased or decreased the combined level of ATP, ADP, and AMP (Fig. 6B). The simulations showed that doubling the adenine pool led to a decrease in the range of ATPase rates where the model can maintain most of the adenine pools in the form of ATP from 9-fold to 4-fold. While halving the adenine pool led to the increase of the supported ATPase range from 9-fold to 13-fold. The effect of adenine pool size on ATP level maintenance can be understood by considering that the activity of HK and PFK is in part controlled by their K_M for ATP. High adenine pool size leads to higher ATP levels and increases the activity of HK and PFK, which improves ATP level maintenance at high ATPase rates and deteriorates it at low ATPase rates. Thus, adjusting the size of the adenine pool is a strategy that cells could use to selectively improve ATP level maintenance at high or low ATPase rates without changing enzyme levels.

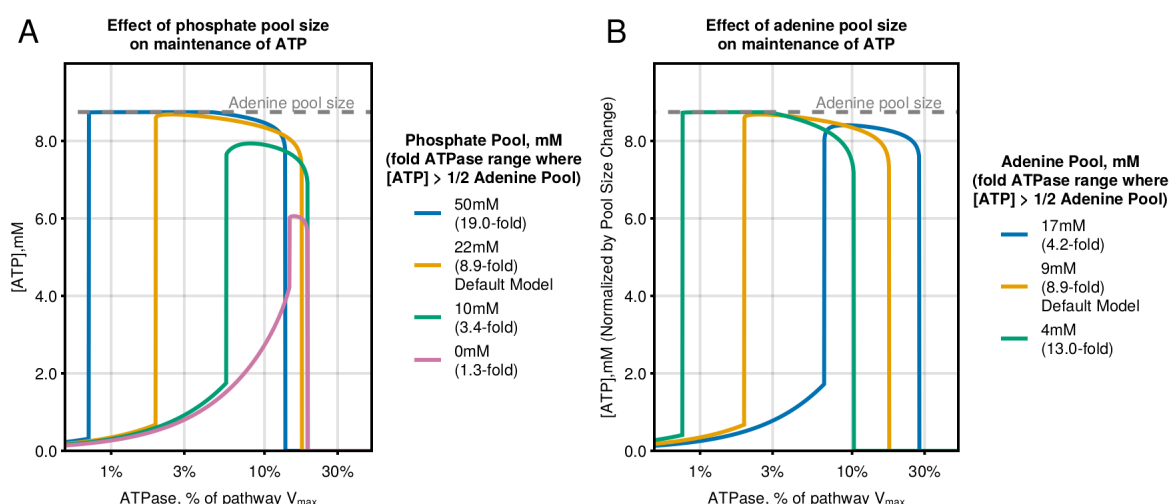


Fig. 6. Large pool of inorganic phosphate is required for maintenance of stable ATP levels. (A) Effect of different amounts of phosphate pool (excluding ATP, ADP, and AMP) on ATP concentration maintenance at different ATPase rates. (B) Effect of increasing or decreasing adenine nucleotide pool on ATP concentration maintenance at different ATPase rates. The dashed grey line indicates the total adenine pool size (i.e., ATP + ADP + AMP). The fold range

of ATPase rates where the model can maintain >50% of the adenine nucleotide pool as ATP is highlighted in figure legends. Julia code to reproduce this figure is available at <https://github.com/DenisTitovLab/Glycolysis.jl>.

Discussion

Allosteric regulation in metabolism has historically been studied by rigorously characterizing enzymes in isolation. While this has greatly advanced our understanding of the key regulatory enzymes involved in this pathway, many emergent properties of metabolism are difficult to understand by focusing on one enzyme at a time. Novel approaches that combine theory and experiment are needed to advance our understanding of metabolic regulation. Here, we describe a data-driven model of glycolysis that harnesses a core of enzymatic rate equations and is fueled by a broad swath of *in vitro* activity data. Our model contains kinetic and thermodynamic parameters describing the activity and allosteric regulation of all glycolytic enzymes through a system of ODEs, and it can predict the output of glycolysis under numerous conditions as described above.

Allosteric regulators of glycolysis are postulated to play an important role in regulating ATP production, but their specific functions remain poorly understood and could involve matching ATP supply and demand, maintaining high energy of ATP hydrolysis to drive cellular processes (i.e., ensuring that the ATPase reaction is maintained far from equilibrium), maintaining high and stable concentrations of ATP such that most of the adenine nucleotide pool is in the form of ATP (i.e., ensuring that enzymes requiring ATP are not kinetically blocked due to low concentrations of ATP), or achieving rapid changes of ATP production in response to sudden changes in ATP demand. Our framework suggests that allosteric regulators are exclusively required to maintain high and stable ATP levels. Indeed, we explicitly show *in silico* that a glycolysis pathway that lacks all allosteric regulation can perform all the functions above except for maintaining most of the adenine nucleotide pool in the form of ATP.

A key advantage of a mechanistic model of glycolysis is that it enables us to computationally dissect the effects of adding or removing any component in the pathway. Analysis of our model has provided explanations for several observed experimental phenomena and yielded multiple predictions that will require experimental follow-up. For example, our analysis revealed that allosteric control of HK1 and PFKP is specifically required to maintain most of the adenine nucleotide pool in the form of ATP, providing an explanation for the evolution of HK1 and PFKP as the sites of allosteric regulation across all domains of life. Surprisingly, allosteric regulation of HK1 and PFKP is predicted to be dispensable for the ability of aerobic glycolysis to match ATP supply and demand or maintain the high energy of ATP hydrolysis. This result predicts that cells expressing non-allosteric mutants of HK1 and PFKP will have a clear defect in their ability to maintain most of their adenine pool in the form of ATP but should still be capable of producing ATP and will likely be viable under some conditions. To the best of our knowledge, the latter experiment has never been attempted. In addition, our model predicts that enzymes of lower glycolysis such as GAPDH, PKM2, and LDH should be as active as possible in relation to HK1 and PFKP to allow glycolysis to maintain most of its adenine pool in the form of ATP explaining why enzymes of lower glycolysis are expressed at more than 10-fold higher levels than HK1 or PFKP (Fig. 5A). Finally, we also find that a pool of inorganic phosphate separate from adenine nucleotide pool is predicted to be important for the ability of glycolysis to maintain most of the adenine nucleotide pool in the form of ATP, which has also not been experimentally tested.

Our model not only confirmed the important role for feedback inhibition by G6P and ATP on glycolytic regulation, but also showed an unexpected role for inorganic phosphate as the key regulator of glycolysis. Phosphate has historically not been considered an important regulator of this pathway, although this role has been proposed in the past (32–34). Mechanistically, phosphate competes with G6P and ATP for the same binding sites and thus serves to inhibit these feedback inhibitors while not influencing HK1 and PFKP activity in the absence of G6P and ATP (35, 36). In addition, phosphate is the substrate of the GAPDH enzyme. Phosphate has several properties that we speculate contribute to its proposed role as the key positive regulator of glycolysis. First, it is a small molecule with a dense negative charge, enabling it to compete with negatively charged G6P and ATP at structurally diverse allosteric sites. Second, phosphate is the product of the ATPase reaction, so its level goes up when glycolysis activity should be upregulated in response to an increase in ATPase activity. But, unlike ADP (the other product of the ATPase reaction), the amount of phosphate is not limited by the adenine pool size, and phosphate levels can increase much more than ADP or AMP. We hypothesize that one of the roles of the creatine phosphate pool is to allow for a dramatic rise in phosphate levels in response to a small change in ATP concentration in order to help maintain ATP homeostasis.

To end, we highlight that the same conceptual framework used here for aerobic glycolysis can be similarly applied to other metabolic pathways. The core of our model is *in vitro* rate equations for each of the glycolytic enzymes, and as long as these equations are available or can be derived for another pathway, the ability to weave them together into a comprehensive systems-level description will be identical to what was described here. Enzyme rate equations that we derived for glycolytic enzymes can be used to describe most metabolic enzymes simply by changing the names of products and substrates and fitting them to *in vitro* kinetics data. We hope that this work will encourage more research on allosteric regulation from both theoreticians and experimentalists, as much more analysis and experimental testing can be done than what was covered in this article.

References and Notes

1. M. Jain, R. Nilsson, S. Sharma, N. Madhusudhan, T. Kitami, A. L. Souza, R. Kafri, M. W. Kirschner, C. B. Clish, V. K. Mootha, Metabolite profiling identifies a key role for glycine in rapid cancer cell proliferation. *Science*. **336**, 1040–1044 (2012).
2. R. J. DeBerardinis, N. S. Chandel, We need to talk about the Warburg effect. *Nature Metabolism*. **2**, 127–129 (2020).
3. M. P. King, G. Attardi, Human cells lacking mtDNA: repopulation with exogenous mitochondria by complementation. *Science*. **246**, 500–503 (1989).
4. D. V. Titov, V. Cracan, R. P. Goodman, J. Peng, Z. Grabarek, V. K. Mootha, Complementation of mitochondrial electron transport chain by manipulation of the NAD⁺/NADH ratio. *Science*. **352**, 231–235 (2016).
5. P. S. Allen, G. O. Matheson, G. Zhu, D. Gheorgiu, R. S. Dunlop, T. Falconer, C. Stanley, P. W. Hochachka, Simultaneous ³¹P MRS of the soleus and gastrocnemius in Sherpas during graded calf muscle exercise. *Am J Physiol*. **273**, R999–1007 (1997).

6. R. S. Balaban, H. L. Kantor, L. A. Katz, R. W. Briggs, Relation between work and phosphate metabolite in the in vivo paced mammalian heart. *Science*. **232**, 1121–1123 (1986).
7. R. Milo, R. Phillips, *Cell Biology by the Numbers* (Garland Science, New York, NY, 1st edition., 2015).
- 5 8. E. E. Sel'kov, Stabilization of energy charge, generation of oscillations and multiple steady states in energy metabolism as a result of purely stoichiometric regulation. *Eur J Biochem*. **59**, 151–157 (1975).
9. T. A. Rapoport, M. Otto, R. Heinrich, An extended model of the glycolysis in erythrocytes. *Acta Biol Med Ger*. **36**, 461–468 (1977).
- 10 10. Y. Termonia, J. Ross, Oscillations and control features in glycolysis: numerical analysis of a comprehensive model. *Proc Natl Acad Sci U S A*. **78**, 2952–2956 (1981).
11. A. Joshi, B. O. Palsson, Metabolic dynamics in the human red cell. Part IV--Data prediction and some model computations. *J Theor Biol*. **142**, 69–85 (1990).
12. B. Teusink, B. M. Bakker, H. V. Westerhoff, Control of frequency and amplitudes is shared by all enzymes in three models for yeast glycolytic oscillations. *Biochim Biophys Acta*. **1275**, 204–212 (1996).
- 15 13. P. J. Mulquiney, P. W. Kuchel, Model of 2,3-bisphosphoglycerate metabolism in the human erythrocyte based on detailed enzyme kinetic equations: equations and parameter refinement. *Biochem J*. **342 Pt 3**, 581–596 (1999).
- 20 14. B. Teusink, J. Passarge, C. A. Reijenga, E. Esgalhado, C. C. van der Weijden, M. Schepper, M. C. Walsh, B. M. Bakker, K. van Dam, H. V. Westerhoff, J. L. Snoep, Can yeast glycolysis be understood in terms of in vitro kinetics of the constituent enzymes? Testing biochemistry. *Eur J Biochem*. **267**, 5313–5329 (2000).
- 25 15. F. Hynne, S. Danø, P. G. Sørensen, Full-scale model of glycolysis in *Saccharomyces cerevisiae*. *Biophys Chem*. **94**, 121–163 (2001).
16. F. A. Chandra, G. Buzi, J. C. Doyle, Glycolytic oscillations and limits on robust efficiency. *Science*. **333**, 187–192 (2011).
17. K. van Eunen, J. A. L. Kiewiet, H. V. Westerhoff, B. M. Bakker, Testing Biochemistry Revisited: How In Vivo Metabolism Can Be Understood from In Vitro Enzyme Kinetics. *PLOS Computational Biology*. **8**, e1002483 (2012).
- 30 18. K. Smallbone, H. L. Messiha, K. M. Carroll, C. L. Winder, N. Malys, W. B. Dunn, E. Murabito, N. Swainston, J. O. Dada, F. Khan, P. Pir, E. Simeonidis, I. Spasić, J. Wishart, D. Weichart, N. W. Hayes, D. Jameson, D. S. Broomhead, S. G. Oliver, S. J. Gaskell, J. E. G. McCarthy, N. W. Paton, H. V. Westerhoff, D. B. Kell, P. Mendes, A model of yeast glycolysis based on a consistent kinetic characterisation of all its enzymes. *FEBS Lett*. **587**, 2832–2841 (2013).
- 35

19. J. H. van Heerden, M. T. Wortel, F. J. Bruggeman, J. J. Heijnen, Y. J. M. Bollen, R. Planqué, J. Hulshof, T. G. O'Toole, S. A. Wahl, B. Teusink, Lost in transition: start-up of glycolysis yields subpopulations of nongrowing cells. *Science*. **343**, 1245114 (2014).
20. A. A. Shestov, X. Liu, Z. Ser, A. A. Cluntun, Y. P. Hung, L. Huang, D. Kim, A. Le, G. Yellen, J. G. Albeck, J. W. Locasale, Quantitative determinants of aerobic glycolysis identify flux through the enzyme GAPDH as a limiting step. *Elife*. **3** (2014), doi:10.7554/eLife.03342.
21. B. C. Mulukutla, A. Yongky, P. Daoutidis, W.-S. Hu, Bistability in Glycolysis Pathway as a Physiological Switch in Energy Metabolism. *PLOS ONE*. **9**, e98756 (2014).
22. J. Monod, J. Wyman, J.-P. Changeux, On the nature of allosteric transitions: A plausible model. *Journal of Molecular Biology*. **12**, 88–118 (1965).
23. D. E. Koshland, G. Némethy, D. Filmer, Comparison of Experimental Binding Data and Theoretical Models in Proteins Containing Subunits*. *Biochemistry*. **5**, 365–385 (1966).
24. S. Marzen, H. G. Garcia, R. Phillips, Statistical Mechanics of Monod–Wyman–Changeux (MWC) Models. *Journal of Molecular Biology*. **425**, 1433–1460 (2013).
25. T. Einav, L. Mazutis, R. Phillips, Statistical Mechanics of Allosteric Enzymes. *J Phys Chem B*. **120**, 6021–6037 (2016).
26. R. Phillips, *The Molecular Switch* (Princeton University Press, 2020; <https://press.princeton.edu/books/hardcover/9780691200248/the-molecular-switch>).
27. M. E. Beber, M. G. Gollub, D. Mozaffari, K. M. Shebek, A. I. Flamholz, R. Milo, E. Noor, eQuilibrator 3.0: a database solution for thermodynamic constant estimation. *Nucleic Acids Res*. **50**, D603–D609 (2022).
28. DifferentialEquations.jl – A Performant and Feature-Rich Ecosystem for Solving Differential Equations in Julia, (available at <https://openresearchsoftware.metajnl.com/articles/10.5334/jors.151/>).
29. J. Bezanson, A. Edelman, S. Karpinski, V. B. Shah, Julia: A Fresh Approach to Numerical Computing. *arXiv:1411.1607 [cs]* (2015) (available at <http://arxiv.org/abs/1411.1607>).
30. M. K. Transtrum, B. B. Machta, K. S. Brown, B. C. Daniels, C. R. Myers, J. P. Sethna, Perspective: Sloppiness and emergent theories in physics, biology, and beyond. *J. Chem. Phys*. **143**, 010901 (2015).
31. A. Saltelli, *Global Sensitivity Analysis: The Primer* (Wiley-Interscience, Chichester, England ; Hoboken, NJ, 1st edition., 2008).
32. K. Uyeda, E. Racker, Regulatory mechanisms in carbohydrate metabolism. 8. The regulatory function of phosphate in glycolysis. *J Biol Chem*. **240**, 4689–4693 (1965).

33. S. C. Rizzo, R. E. Eckel, Control of glycolysis in human erythrocytes by inorganic phosphate and sulfate. *Am J Physiol.* **211**, 429–436 (1966).
34. S. Minakami, H. Yoshikawa, Studies on erythrocyte glycolysis. 3. The effects of active cation transport, pH and inorganic phosphate concentration on erythrocyte glycolysis. *J Biochem.* **59**, 145–150 (1966).
35. B. A. Webb, F. Forouhar, F.-E. Szu, J. Seetharaman, L. Tong, D. L. Barber, Structures of human phosphofructokinase-1 and atomic basis of cancer-associated mutations. *Nature.* **523**, 111–114 (2015).
36. X. Liu, C. S. Kim, F. T. Kurbanov, R. B. Honzatko, H. J. Fromm, Dual Mechanisms for Glucose 6-Phosphate Inhibition of Human Brain Hexokinase *. *Journal of Biological Chemistry.* **274**, 31155–31159 (1999).

Acknowledgments: We thank the students and instructors of the Marine Biological Laboratory course on Physical Biology of the Cell for their comments on the early version of this project; participants of the Kavli Institute for Theoretical Physics workshop on Cellular Energetics for fruitful discussions; Bradley Webb for discussions about PFK regulation; and members of Titov and Phillips labs for helpful suggestions. This research used the Savio computational cluster resource provided by the Berkeley Research Computing program at the University of California, Berkeley (supported by the UC Berkeley Chancellor, Vice Chancellor for Research, and Chief Information Officer).

Funding:

National Institutes of Health grant DP2 GM132933 (DVT)

National Institutes of Health grant 5R35 GM118043-7 (RP)

Damon Runyon Cancer Research Foundation Fellowship DRQ 01-20 (TE)

Author contributions:

Conceptualization: RP, DVT

Data curation: MC, TE, DVT

Methodology: MC, TE, DVT

Investigation: MC, TE, DVT

Funding acquisition: RP, DVT

Supervision: RP, DVT

Writing – original draft: DVT

Writing – review & editing: MC, TE, RP, DVT

Competing interests: Authors declare that they have no competing interests.

Data and materials availability: All data are available in the main text or the supplementary materials. The Julia code for the glycolysis model that reproduces all the figures in the main text is deposited at <https://github.com/DenisTitovLab/Glycolysis.jl>.

Supplementary Materials

Materials and Methods

Supplementary Text

Figs. S1 to S13

5 Tables S1 to S13

References

Data S1 to S2